

# Damped Lyman Alpha Systems at High Redshift and Models of Protogalactic Disks

Karsten Jedamzik<sup>1</sup> *and* Jason X. Prochaska<sup>2</sup>

<sup>1</sup>Max-Planck-Institut für Astrophysik

85740 Garching bei München

<sup>2</sup> Department of Physics, and Center for Astrophysics and Space Sciences,

University of California, San Diego

We employ observationally determined intrinsic velocity widths and column densities of damped Lyman-alpha systems at high redshift to investigate the distribution of baryons in protogalaxies within the context of a standard cold dark matter model. We proceed under the assumption that damped Lyman alpha systems represent a population of cold, rotationally supported, protogalactic disks and that the abundance of dark matter halos is well approximated by a cold dark matter model with critical density and vanishing cosmological constant. Using conditional cross sections to observe a damped system with a given velocity width and column density, we compare observationally inferred velocity width and column density distributions to the corresponding theoretically determined distributions for a variety of disk parameters and CDM normalizations. In general, we find that the observations can not be reproduced by the models for most disk parameters and CDM normalizations. Whereas the column density distribution favors small disks with large neutral gas fraction, the velocity width distribution favors large and thick disks with small neutral gas fraction. The possible resolutions of this problem in the context of this CDM model may be: (1) an increased contribution of rapidly rotating disks within massive dark matter halos to damped Lyman-alpha absorption or (2) the abandoning of simple disk models

within this CDM model for damped Lyman-alpha systems at high redshift. Here the first possibility may be achieved by supposing that damped Lyman-alpha system formation only occurs in halos with fairly large circular velocities and the second possibility may result from a large contribution of mergers and double-disks to damped Lyman-alpha absorption at high redshift.

# 1 Introduction

It is widely believed that the phenomena of damped Lyman-alpha (hereafter; damped Ly- $\alpha$ ) absorption in the spectra of high redshift quasars is due to large amounts of neutral gas in dark matter halos which intervene on the lines of sight to quasars [Wolfe et al. 1986]. It is intriguing that the ratio of neutral gas mass density to the critical density in damped Ly- $\alpha$  systems,  $\Omega_{Ly\alpha}(z)$ , at redshift  $z \sim 3$  is comparable to the baryonic content of stars in galaxies at the present epoch [Lanzetta et al. 1995, Wolfe et al. 1995]. Both the steady decline in  $\Omega_{Ly\alpha}(z)$  with decreasing redshift and the agreement between  $\Omega_{Ly\alpha}(z)$  at low  $z$  and the neutral gas content of nearby galaxies [Rao & Briggs 1993] are commonly interpreted as the incorporation of baryons into stars within the damped systems [Lanzetta et al. 1995, Wolfe et al. 1995]. Observations of damped Ly- $\alpha$  systems have, and continue, to yield important information about the abundances and masses of dark matter halos, as well as the process of star formation [Ma and Bertschinger 1994, Kauffmann and Charlot 1994, Mo & Miralda-Escoude 1994].

Whereas the hosts of damped Ly- $\alpha$  systems seem to be established, there is considerable debate about the distribution of neutral gas in individual dark matter halos at high redshift. For example, neutral gas in damped Ly- $\alpha$  systems may be distributed spherically symmetric within the halo, or may be within a rotationally supported protogalactic disk. The main observational support for damped Ly- $\alpha$  systems representing halo gas comes from a comparison of metallicities of damped Ly- $\alpha$  systems as a function of redshift with the metallicities of disk and halo stars as a function of stellar age [Pettini et al. 1994, Lu et al. 1996]. On the other hand, there is accumulating observational evidence that damped Ly- $\alpha$  systems at high redshift are protogalactic disks. Prochaska & Wolfe (1997a; hereafter PW) recently analyzed a sample of 17 damped Ly- $\alpha$  systems observed at high-resolution with HIRES on the Keck I telescope. They argue that observationally determined velocity profiles of high-redshift damped systems are reflective of rapidly rotating, cold disks, and cannot be reconciled with isothermal halo gas models or slowly rotating “hot” disks. In addition, the recent

observation of the stellar and continuum emission of a high-redshift galaxy believed to be responsible for damped Ly- $\alpha$  absorption in the spectrum of a quasar may be explained straightforwardly only if one assumes the galaxy to be host of a disk [Djorgovski et al. 1996, Lu et al. 1997].

Unfortunately it is not possible to easily obtain a resolution to the debate about the spatial and velocity distribution of neutral gas in dark matter halos from numerical simulations. This is partially due to limited resolution, such that simulations which contain enough halos to be statistically representative may not resolve the physics within an individual halo [Gardner et al. 1997]. Furthermore, when simulating the formation of disks in individual halos within the context of currently popular structure formation scenarios, the sizes of disks are predicted to be much smaller than the observationally inferred sizes of present day galaxies, casting significant doubt on the predictive power of the simulations [Navarro, Frenk & White 1995]. Nevertheless, numerical simulations may shed further light on the nature of damped Ly- $\alpha$  systems; for example, they may test if it is realistic to employ simple models for the velocity distribution of gas or if, rather, the occurrence of damped systems results from cold, rotating disks, as well as halo gas, merging galaxies, and/or irregular galaxies in almost equal parts [Haehnelt et al. 1997].

Semianalytic models for the formation of disk galaxies are very successful in explaining properties of present-day spiral galaxies [Fall & Efstathiou 1980, Kauffmann 1996, Dalcanton et al. 1997, Mo et al. 1997]. These models consist of two parts, a Press-Schechter type formalism to determine the abundances and masses of halos in a given hierarchical structure formation scenario, and a model for the formation of a rotationally supported disk within the dark halo. The sizes and profiles of disks may be estimated by the distribution of halo angular momentum under the assumption that there is no angular momentum transport between halo and disk, and that baryons are initially in solid body rotation. When combined with efficiencies to turn gas into stars, such models successfully explain the observed trends and scatter in exponential disk scale length, surface brightness, and the Tully-Fisher relationship [Dalcanton et al. 1997, Mo et al. 1997].

It is instructive to see if such disk models may also reproduce the observational data of damped Ly- $\alpha$  systems at high redshift. In fact, an initial, not fully self-consistent, comparison between the observational data and one particular disk formation model [Kauffmann 1996] demonstrated that there is significant discrepancy between the model and the observations (PW).

In this paper we compare observationally inferred velocity widths of a sample of damped Ly- $\alpha$  systems at mean redshift  $z \approx 3$  to theoretically predicted velocity widths for a variety of disk models. In Section 2 we summarize the assumptions entering our calculation of halo abundances and masses, as well as disk rotational velocities. We also describe our computation of conditional cross sections, to observe a disk with more than the critical column density for a damped system and a velocity width more than a certain fraction of the rotational velocity of the disk. Our results and conclusions are presented in Section 3.

## 2 Semianalytic Model of Protogalactic Disk Populations

We consider the conditional optical depth per unit redshift,  $d\tau/dz(\Delta v_{th})$ , for observing a damped Ly- $\alpha$  system showing a velocity spread,  $\Delta v$ , larger than some threshold,  $\Delta v_{th}$ . Note that the optical depth per unit redshift is frequently called the rate of incidence. The conditional optical depth is the product of proper number density of halos hosting damped systems, the conditional cross section for observing a damped system with velocity spread larger than  $\Delta v_{th}$ , and the proper path length traveled by a photon per unit redshift interval, i.e.  $d\tau/dz = n^p \sigma_d dl^p/dz$ . We assume that the kinematics and gas distribution of damped Ly- $\alpha$  systems is adequately described by rotationally supported disks within dark matter halos. To account for a continuous distribution of halo masses we use the Press-Schechter formalism for halo formation with density threshold  $\delta_c = 1.68$  and top hat filter. In our calculations we assume that the abundances of halos are well approximated by the abundances in a closed cold dark matter model with vanishing cosmological constant and varying normalizations. We use the CDM transfer function by Bardeen *et al.* (1986) with scale

invariant initial perturbations ( $n = 1$ ) and Hubble parameter  $H_0 = 50 \text{ km s}^{-1} \text{ Mpc}^{-1}$  ( $h = 0.5$ ).

The conditional optical depth for a continuous mass distribution may be written as

$$\frac{d\tau}{dz}(\Delta v_{th}) = \frac{c}{H_0} (1+z)^{-5/2} \int_{M(v_c^{min})}^{\infty} dM \frac{dn^p(M)}{dM} \sigma_d(M, \Delta v_{th}), \quad (1)$$

with  $c$  the speed of light. Note that we will use an equation similar to Eq. 1 for the computation of column density distributions where the conditional disk cross section in Eq. 1 is replaced by an adequate column density distribution. In writing Eq. 1 we assume that damped systems only form within sufficiently large halos with circular velocities exceeding a minimum value,  $v_c^{min}$ . Even though it has been argued on physical grounds that  $v_c^{min} \approx 35-50 \text{ km s}^{-1}$  due to photoionization by the UV-background at high redshift and the associated long cooling time scales for baryons in small halos [Efstathiou 1992], we will treat  $v_c^{min}$  as a free parameter in order to assess the contribution of less massive halos to the conditional optical depth.

We may parametrize the conditional disk cross section by

$$\sigma_d(M, \Delta v_{th}) = \pi R_d^2 F(N_{\perp}, \kappa \mid N \geq N_d, f_v = \Delta v / v_{rot} \geq \Delta v_{th} / v_{rot}), \quad (2)$$

where  $R_d$ ,  $N_{\perp}$ ,  $\kappa$ , and  $v_{rot}$  are scale length, central column density, ratio of scale height to scale length, and rotational velocity of the disk, respectively. The cross section receives only contributions from lines of sight which (1) result in column densities  $N$  exceeding the threshold for a damped system  $N_d = 2 \times 10^{20} \text{ cm}^{-2}$  and (2) show velocity width  $\Delta v = f_v v_{rot}$  exceeding the velocity width threshold,  $\Delta v_{th}$ . Note that due to the self-similarity of disks with different  $R_d$  but the same  $N_{\perp}$  and  $\kappa$ , the function  $F$  depends explicitly only on  $N_{\perp}$  and  $\kappa$ , but not  $R_d$ , provided one assumes a flat rotation curve. We assume the disk rotational velocity equals the circular velocity of the halo

$$v_{rot} = v_c = \sqrt{\frac{GM}{r_{vir}}} = 159.6 \frac{\text{km}}{\text{s}} h^{1/3} \left( \frac{M}{10^{12} M_\odot} \right) (1+z)^{1/2}. \quad (3)$$

Here  $r_{vir}$  is the virial radius of a halo calculated within the spherical collapse model, and  $G$  is the gravitational constant. Motivated by the successes of semianalytic formation models of present-day disk galaxies, we assume that the scale length of the disk is proportional to the virial radius of the halo

$$R_d = f r_{vir} = \frac{f}{(179)^{1/3}} \left( \frac{3M}{4\pi\rho_0} \right)^{1/3} \frac{1}{(1+z)} = 169.7 \text{kpc} f \frac{h^{-2/3}}{(1+z)} \left( \frac{M}{10^{12} M_\odot} \right)^{1/3}. \quad (4)$$

In order to evaluate conditional disk cross sections, we make several simplifying assumptions regarding the physical characteristics of the disks. We adopt a simple, phenomenologically motivated disk model, the exponential disk. As in PW, we parameterize the neutral gas density of the disk,  $n_H$ , by

$$n_H(R, Z) = n_0 \exp \left[ -\frac{R}{R_d} - \frac{|Z|}{\kappa R_d} \right], \quad (5)$$

where  $n_0$  is the central gas density. Furthermore, we describe the gas kinematics by a flat rotation curve, parameterized by the rotation speed,  $v_{rot}$ , and a random motion component characterized by a 1-dimensional velocity dispersion,  $\sigma = 10 \text{ km s}^{-1}$ . Conserving baryonic mass within halos, the central column density may be related to the total halo mass by

$$N_\perp = \int n_H(0, Z) dZ = 2n_0 \kappa R_d = \frac{f_N \Omega_b M}{\mu m_H 2\pi R_d^2}, \quad (6)$$

where  $m_H$  is the hydrogen mass,  $\Omega_b = 0.05$  is the assumed fractional contribution of baryons to the critical density, and  $\mu \approx 1.3$  accounts for the fact that a fraction of all baryons are in form of

helium. The parameter  $f_N \leq 1$  is the fraction of baryons participating as neutral gas in the disk. This fraction may be smaller than one if either there is an ionized component of gas due to partial photoionization or if gas is efficiently incorporated into stars.

In order to calculate the cross section  $\sigma_d(M, \Delta v_{th})$  we consider two conditional cross-sections: (1)  $\sigma_{NHI}$ , defined as the cross-section for sightlines yielding column densities  $N(\text{HI}) \geq 2 \times 10^{20} \text{ cm}^{-2}$  (the damped Ly $\alpha$  threshold), and (2) the conditional velocity width cross-section,  $\sigma_{f_c}$ , for sightlines which give a velocity width,  $\Delta v$ , greater than a fraction,  $f_c$ , of the rotation speed ( $f_c \in [0, 1]$ ). We calculate  $\sigma_{f_c}$  and  $\sigma_{NHI}$  by systematically running sightlines through an exponential disk according to the techniques outlined in §3.2 of PW. While computer intensive, the process is straightforward and reproducible. To verify the accuracy of our procedures we compare  $\sigma_{NHI}$  with the cross-sections determined by Fall & Pei (1993) in the thin-disk limit and find excellent agreement over the whole column density range  $N_{\perp} = 10^{18.9} - 10^{23.9} \text{ cm}^{-2}$ . Note also that we find the thin-disk limit to be an excellent approximation to  $\sigma_{NHI}$  even for finite thickness disks ( $\kappa \sim 0.5$ ). To simplify the computations, we make use of the fact that  $\sigma_{f_c}$  is independent of  $N_{\perp}$ . We may then obtain the doubly conditional cross section  $\sigma_d$  for given  $N_{\perp}$ ,  $\kappa$  and  $f_c$  by convolving the cross-sectional area leading to  $\sigma_{NHI}$  with the cross-sectional area leading to  $\sigma_{f_c}$ .

The doubly conditional cross-section depends on the disk parameters in the following ways. Thicker disks (larger  $\kappa$  values) imply larger velocity widths and therefore larger  $\sigma_d$  for a given  $f_c$  value due to the increased path length of sightlines within the disk. The dependence of  $\sigma_d$  on  $N_{\perp}$  is more complicated. As noted in PW (e.g. Figure 3), the velocity widths tend to decrease with larger impact parameters for a given sightline. This is primarily because the differential rotation projected along the line of sight decreases with increasing impact parameter. For a disk with a large  $N_{\perp}$  value even sightlines at a number of scale lengths may lead to the observation of a damped system. However, due to the large impact parameter such sightlines only yield fairly small  $\Delta v/v_{rot}$ . These ideas are illustrated in Figure 1 where we plot  $\sigma_d$  for two different  $N_{\perp} = 10^{20.5}, 10^{22.1} \text{ cm}^{-2}$

and  $\kappa = 0.108, 0.232$  as a function of  $f_c$ , and where  $\sigma_d = \sigma_{NHI}$  for  $f_c \leq 0.05$ . It is essential for the conclusions of this paper that we find only a small fraction  $\sim 1/10$  of sightlines which result into the observation of a damped system also show more than  $\sim 50\%$  of the rotation velocity for large  $N_\perp$  disks. This is not the case for small  $N_\perp$  disks where this ratio is approximately one-half.

### 3 Results

Given the results from §2, we can calculate the optical depth per unit redshift,  $d\tau/dz$ , for damped Ly $\alpha$  systems showing more than a certain velocity width,  $\Delta v_{th}$ , as a function of  $\Delta v_{th}$ . The model has 5 free parameters: (1)  $\sigma_8$ , the linear rms fluctuation amplitude measured at  $8 \text{ h}^{-1} \text{ Mpc}$ , (2)  $v_c^{min}$ , the circular velocity cutoff corresponding to the least massive dark matter halo capable of forming a damped system, (3)  $\kappa$ , the ratio of the scale height to the scale length, (4)  $f$ , the scale length of the disks as a fraction of the virial radius, and (5)  $f_N$ , the fraction of baryons within a dark matter halo which contribute to the disk. In Figures 2a-e we compare optical depth curves calculated over a wide range of the physically allowed parameter space with  $d\tau/dz$  measured from 26 damped Ly $\alpha$  systems with redshifts  $z = 2.0 - 4.4$  ( $\bar{z} = 2.86$ ). Fourteen of the systems were presented in PW and the remaining 12 can be found in Prochaska & Wolfe (1997b). The sample is kinematically unbiased and each system has an accurately determined velocity width.

Figures 2a and 2b present the effects of  $\sigma_8$  and  $v_c^{min}$ , respectively, on the predicted optical depth. These two parameters determine the number density of halos as a function of circular velocity. In particular, by increasing  $\sigma_8$  and/or  $v_c^{min}$  the mass function of halos capable of forming damped systems is shifted towards halos with larger  $v_c$ , and disks with larger  $v_{rot}$ . In panel (a) we consider a range of  $\sigma_8$  values, including the two most favored observational values:  $\sigma_8 = 0.667$  from the observed masses of rich clusters [White, Efstathiou, & Frenk 1993] and  $\sigma_8 = 1.2$ , the normalization implied by measurements of the CMBR [Gorski et al. 1996]. First note that none of the  $d\tau/dz$  curves in panel (a) are consistent with the observational data. Whereas the observations

indicate that a fraction of one-half of all damped systems show an intrinsic velocity width of  $\Delta v \geq 100 \text{ km s}^{-1}$  our models show that this fraction is  $\leq 1/10$  for  $\sigma_8 \leq 1$ . Note that we choose  $f = 0.1$  and  $f_N = 1$  in panel (a) yielding typical central column densities of  $N_{\perp} \sim 10^{22} \text{ cm}^{-2}$ . The small fraction of large  $\Delta v$  systems in our model is then due almost in equal parts to a comparatively large fraction of small  $v_c$  systems as well as due to the small chance for observing a significant fraction of the rotational velocity at such high  $N_{\perp}$  (cf. Fig. 1). It is evident from panel (b) that by removing the contributions of small halos ( $v_c \leq 200 \text{ km s}^{-1}$ ) to the optical depth one may obtain approximate agreement between observations and the model. This highlights the fact that the CDM model with  $\sigma_8 \approx 1$  predicts enough massive halos ( $v_c \geq 200 - 300 \text{ km s}^{-1}$ ) at high redshift to account for the abundance of damped systems with large intrinsic velocity width.

The dependence of the optical depth on the parameters  $\kappa$ ,  $f$  and  $f_N$  which affect the cross-section of the disks within the dark matter halos, is shown in panels (c)–(e). In Figure 2c we plot  $d\tau/dz$  against  $\Delta v$  for models with varying disk thickness. It is seen that the observational data favors thick disks and that disks with thicknesses comparable to the thin disk of the Milky Way ( $\kappa \approx 0.05$ ; Mihalas & Binney 1981) are unacceptable. We investigate the effect of varying the disk size in panel (d). One may produce a nearly acceptable fit of the velocity distribution data even for low normalization CDM models ( $\sigma_8 = 0.5$ ) by taking the scale length of the disks to be a considerable fraction of the virial radius ( $f \approx 0.8$ ). Agreement between the model predictions for the velocity width distribution and the observations is then attained due to the comparatively large typical fraction of the rotational velocity one observes in these low central column density ( $N_{\perp} \sim 10^{20.3} \text{ cm}^{-2}$ ) systems (cf. Fig. 1). It is important to stress that analytic models of disks within a CDM cosmogony (e.g. Dalcanton et al. 1997, Mo et al. 1997) suggest  $f \approx \bar{\lambda}$ , the average spin angular momentum parameter which has been measured numerically to be  $\bar{\lambda} \approx 0.05 \pm 0.03$  [Barnes & Efstathiou 1987]. Such analytic models are thus inconsistent with extremely large scale length  $R_d$ . Finally, we allow for the possibility that not all of the baryons within the halos will

collapse to form a gaseous disk. Numerical simulations suggest [Ma et al. 1997] that a fraction of baryons in halos will remain hot due to photoionization by the UV-background and therefore not contribute to damped Ly $\alpha$  absorption. Moreover, it is possible that a significant fraction of baryons may be incorporated into stars by a redshift of  $z \approx 2.5$ . As is evident from panel (e) in Fig. 2, lowering  $f_N$  has the effect of increasing the fraction of high  $\Delta v$  systems, thereby slightly lessening the discrepancy between model and observations. This is again due to a decrease in the average central column densities of disks.

Nevertheless, disks with low central column densities are inconsistent with the column density distribution for damped Ly $\alpha$  systems at high redshift. In Fig. 3 we compare the column density distribution resulting from several of the models in Fig. 2 to the observationally determined column density distribution at mean redshift  $\bar{z} = 3.0$  [Wolfe et al. 1995]. It is evident from the figure that the observational data clearly favors large  $N_{\perp}$  disks (the dotted and long-dashed lines are models with low average  $N_{\perp}$ ). Significantly increased scale lengths  $R_d$ , or decreased neutral fractions  $f_N$ , are therefore ruled out as an explanation for the comparatively flat velocity width distribution of damped Ly $\alpha$  systems.

While it seems difficult to simultaneously reproduce the velocity width and column density data of damped Ly $\alpha$  systems within the context of simple disk models in a CDM cosmogony, our model has enough parametric freedom to yield an acceptable fit. In Figure 2 (panel f) and Figure 3 (the dashed-dotted line) we show such a model with fairly thick disks ( $\kappa = 0.39$ ), large velocity cutoff ( $v_c^{min} = 150 \text{ km s}^{-1}$ ), and small neutral fraction ( $f_N = 0.33$ ). However, such a fit requires significant “fine tuning” and yields a physically unmotivated model. As such, we believe that simple disk models in a CDM cosmogony cannot reproduce straightforwardly the observational data of damped Ly $\alpha$  systems at high redshift. This is in contrast to the success of such models in explaining the properties of present day spiral galaxies (e.g. Kauffmann 1996). Nevertheless, it is interesting to note that CDM models for the formation of structure, combined with assumptions of

gas cooling and star formation, tend to significantly overproduce the abundances of faint galaxies [White & Frenk 1991]. Though there are alternative explanations to this apparent discrepancy between observations of the present-day luminosity function and the model predictions, one solution would be a suppression of gas cooling and star formation in low circular velocity halos. If cooling of gas in less massive  $v_c \leq 200 \text{ km s}^{-1}$  halos would be similarly suppressed at high redshift, than protogalactic disks within a CDM cosmology would remain as a viable model for the nature of damped Ly $\alpha$  systems at high redshift.

There are two physical effects which have not been taken into account in our model and which could alleviate the discrepancy between the observationally determined velocity width distribution and our model predictions. Mo et al. (1997) compute rotation curves for galactic disks within realistic dark matter halos. They find that low  $v_c$  halos have rotation curves which have a peak of approximate height  $v_{rot} \approx 1.5v_c$ . Since this peak is approximately located at a distance from the disk center where damped Ly $\alpha$  absorption is dominated (at the threshold for damped systems  $N_d$ ) the “effective” rotation velocity of low  $v_c$  halos may exceed  $v_c$ . Further, hydrodynamic simulations employed in the analysis of Ma et al. (1997) indicate that there may be partial ionization of disks at larger distances from the disk center. Lines of sight which penetrate the disk at large impact parameters typically yield only small  $\Delta v$ . If those lines of sight do not contribute to damped Ly $\alpha$  absorption, the average observed  $\Delta v$  of a given disk increases. It remains to be shown if these effects can significantly improve the comparison between the observationally determined velocity width distribution and the disk model predictions.

In summary, we have compared observationally determined velocity width and column density distributions of damped Ly $\alpha$  systems at high redshift to theoretically predicted distributions within the context of protogalactic disk models for damped Ly $\alpha$  systems in a closed CDM model with vanishing cosmological constant. Whereas the column density distribution may be reasonably well reproduced by assuming rotationally supported disks with scale length comparable to those

inferred from successful semianalytic models for the formation of present-day spiral galaxies, the simplest protogalactic disk models cannot reproduce the velocity width distribution. This discrepancy is mainly due to the large fraction of small circular velocity halos within the CDM model. Approximate agreement between the observational data and the disk model predictions may be obtained if the contribution of low circular velocity systems  $v_c \leq 200 \text{ km s}^{-1}$  to damped Ly $\alpha$  absorption is significantly diminished. By increasing the thickness of disks and slightly decreasing the neutral fraction of gas one may further improve the agreement between observational data and the model. Leaving the realm of the model investigated in this paper, there are two alternative solutions to the problem. It may well be that only a fraction of all damped systems are “regular” protogalactic disks. In this case most of the damped Ly $\alpha$  systems which show large intrinsic velocity width  $\Delta v \geq 100 \text{ km s}^{-1}$  have to be the result of damped Ly $\alpha$  absorption resulting from lines of sight through double disks, ongoing mergers, and irregular gas distributions. Since the observed fraction of damped systems with  $\Delta v \geq 100 \text{ km s}^{-1}$  is large ( $\sim 50\%$ ) only a similarly large fraction of such systems at high redshift  $z \approx 3$  may reproduce the observations. Further light on this issue may be shed by hydrodynamical simulations of structure formation [e.g. Haehnelt et al. 1997]. Finally, it may simply be that the CDM models employed in this paper overproduce the abundances of small  $v_c$  halos and do not represent the “correct” structure formation scenario.

We acknowledge many useful discussions with Martin Haehnelt, Houjun Mo, Simon White, and Arthur Wolfe. JXP would especially like to thank W.L.W. Sargent and L. Lu for providing their HIRES spectra. This work was supported by NASA grant NAGW-2119 and NSF grant AST 86-9420443 (JXP) and...

## 4 Figure Captions

**Figure 1**

The doubly conditional cross-section,  $\sigma_d$  in units of  $R_d^2/\pi$  for a disk yielding a velocity width  $\Delta v$  greater than a fraction,  $f_c$ , of the rotation speed for disks with two different central column densities ( $N_{\perp} = 10^{20.5}, 10^{22.1}$ ; top and bottom lines respectively) and thickness ( $\kappa = 0.108, 0.232$ ; dashed and solid lines respectively).

**Figure 2**

Optical depth per unit redshift,  $d\tau/dz$ , for damped Ly- $\alpha$  systems showing a velocity width,  $\Delta v$ , more than a threshold  $\Delta v \geq \Delta v_{th}$ , as a function of  $\Delta v_{th}$ . The observationally determined distribution is shown by  $\pm 1\sigma$  bars for a sample of 26 damped Ly- $\alpha$  systems with mean redshift  $z = 2.87$ . The dotted lines show theoretically determined velocity width distributions at the same redshift for cold, rotating disks in CDM models with Hubble constant  $h = 0.5$  and baryonic contribution to the closure density,  $\Omega_b = 0.05$ . Panel (a) corresponds to models with parameters  $f = 0.108$ ,  $\kappa = 0.232$ ,  $f_N = 1$ ,  $v_c^{min} = 50 \text{ km s}^{-1}$ , and varying CDM normalization  $\sigma_8 = 2, 1, 0.6667, 0.5$  (from top to bottom, respectively), where  $\sigma_8$  is the linear rms fluctuation amplitude on a scale of  $8h^{-1}\text{Mpc}$ ,  $f$  is the exponential disk scale length in units of the halo virial radius,  $\kappa$  is the ratio of scale height to scale length,  $f_N$  is the fraction of baryons contributing to neutral disk gas, and  $v_c^{min}$  is the lowest circular velocity of halos where gas may still cool and form damped Ly- $\alpha$  systems. The remaining panels correspond to models with parameters (b)  $f = 0.108$ ,  $\kappa = 0.232$ ,  $\sigma_8 = 1$ ,  $f_N = 1$ , and varying velocity cutoff  $v_c^{min} = 50, 100, 200, 300 \text{ km s}^{-1}$  (from top to bottom, respectively); (c)  $f = 0.108$ ,  $\sigma_8 = 1$ ,  $f_N = 1$ ,  $v_c^{min} = 50 \text{ km s}^{-1}$ , and varying disk thickness  $\kappa = 0.5, 0.232, 0.108, 0.05$  (from top to bottom, respectively); (d)  $\kappa = 0.232$ ,  $\sigma_8 = 0.5$ ,  $f_N = 1$ ,  $v_c^{min} = 50 \text{ km s}^{-1}$ , and varying disk size  $f = 0.834, 0.5, 0.232, 0.108$  (from top to bottom at high  $\Delta v$ , respectively); (e)  $f = 0.108$ ,  $\kappa = 0.232$ ,  $\sigma_8 = 1$ ,  $v_c^{min} = 50 \text{ km s}^{-1}$ , and varying neutral gas fraction  $f_N = 1, 0.5, 0.25, 0.1$  (from top to bottom, respectively); and (f)  $f = 0.108$ ,  $\kappa = 0.39$ ,

$\sigma_8 = 1$ ,  $v_c^{min} = 150$  km s $^{-1}$ , and  $f_N = 0.33$ .

### Figure 3

Column density distribution for damped Ly- $\alpha$  systems,  $f(N)$ , as a function of  $N$  at mean redshift  $z = 3$ . The crosses show observational data taken from Wolfe et al (1995) with the vertical lines indicating the  $\pm 1\sigma$  ranges. The different lines show theoretically determined column density distributions for some of the models in Figure 2. The lines correspond to model parameters  $f = 0.05$ ,  $\kappa = 0.232$ ,  $\sigma_8 = 1$ ,  $f_N = 1$ , and  $v_c^{min} = 50$  km s $^{-1}$  (solid line);  $f = 0.834$ ,  $\kappa = 0.232$ ,  $\sigma_8 = 2$ ,  $f_N = 1$ , and  $v_c^{min} = 50$  km s $^{-1}$  (dotted line);  $f = 0.108$ ,  $\kappa = 0.232$ ,  $\sigma_8 = 1$ ,  $f_N = 1$ , and  $v_c^{min} = 200$  km s $^{-1}$  (short-dashed line);  $f = 0.108$ ,  $\kappa = 0.232$ ,  $\sigma_8 = 1$ ,  $f_N = 0.1$ , and  $v_c^{min} = 50$  km s $^{-1}$  (long-dashed line); and  $f = 0.108$ ,  $\kappa = 0.39$ ,  $\sigma_8 = 1$ ,  $f_N = 0.33$ , and  $v_c^{min} = 150$  km s $^{-1}$  (dashed-dotted line);

## References

- [Bardeen et al. 1986] Bardeen, J.M., Bond, J.R., Kaiser, N., & Szalay, A.S. 1976, ApJ, 304, 15
- [Barnes & Efstathiou 1987] Barnes, J. & Efstathiou, G. 1987, ApJ, 319, 575
- [Dalcanton et al. 1997] Dalcanton, J.J., Spergel, D.N., & Summers, F.J. 1997, ApJ, 482, 659
- [Djorgovski et al. 1996] Djorgovski, S.G., Pahre, M.A., Bechtold, J., & Elston, R. 1996, Nature, 382, 234
- [Efstathiou 1992] Efstathiou, G. P. 1992, MNRAS, 193, 189
- [Fall & Efstathiou 1980] Fall, S.M. & Efstathiou, G. 1980, MNRAS, 193, 189
- [Fall & Pei 1993] Fall, S.M. & Pei, Y.C. 1993, ApJ, 402, 479
- [Gardner et al. 1997] Gardner, J.P., Katz, N., Hernquist, L. & Weinberg, D.H. 1997, ApJ, in press

[Gorski et al. 1996] Gorski, K.M. et al. 1996, ApJ, 464, L11

[Haehnelt et al. 1997] Haehnelt, M.G., Steinmetz, M. & Rauch, M. 1997, astro-ph 9706201

[Kauffmann and Charlot 1994] Kauffmann, G. & Charlot, S. 1994, ApJ, 430 L97

[Kauffmann 1996] Kauffmann, G. 1996, MNRAS, 281, 475

[Lanzetta et al. 1995] Lanzetta, K. M., Wolfe, A. M., & Turnshek 1995, ApJ, 440, 435

[Lu et al. 1996] Lu, L., Sargent, W.L.W., & Barlow, T.A. 1996, /apj, 107, 475

[Lu et al. 1997] Lu, L., Sargent, W.L.W., & Barlow, T.A. 1997, /apj, in press

[Ma and Bertschinger 1994] Ma, C.-P., & Bertschinger, E. 1994, ApJ, 434, L5

[Ma et al. 1997] Ma, C.-P., Bertschinger, E., Hernquist, L., Weinberg, D.H., & Katz, N. 1997, astro-ph/9705113

[Mihalas & Binney 1981] Mihalas,D. & Binney, J.J. 1981 *Galactic Astronomy*, 2nd ed. San Francisco: Freeman

[Mo & Miralda-Escoude 1994] Mo, H.J., & Miralda-Escoude, J. 1994, ApJ, 430, L25

[Mo et al. 1997] Mo, H.J., Mao, & White, S.D.M. 1997, ??

[Navarro, Frenk & White 1995] Navarro, J.F., Frenk, C.S., & White, S.D.M. 1995, MNRAS, 275, 56

[Pettini et al. 1994] Pettini, M., Smith, L. J., Hunstead, R. W., and King, D. L. 1994, ApJ, 426, 79

[Prochaska and Wolfe 1997a] Prochaska, J. X. and Wolfe, A. M. 1997, ApJ, 48

[Prochaska and Wolfe 1997b] Prochaska, J. X. and Wolfe, A. M. 1997, in preparation

[Rao & Briggs 1993] Rao, S. & Briggs, F.H. 1993, ApJ, 419, 515

[White & Frenk 1991] White, S.D.M., & Frenk, C.S. 1991, ApJ, 379, 52

[White, Efstathiou, & Frenk 1993] White, S.D.M, Efstathiou, G., & Frenk, C.S. 1993, MNRAS, 262, 1023

[Wolfe et al. 1986] Wolfe, A.M., Turnshek, D.A., Smith, H.E., & Cohen, R.D. 1986, ApJS, 61, 249

[Wolfe et al. 1995] Wolfe, A. M., Lanzetta, K. M., Foltz, C. B., and Chaffee, F. H. 1995, ApJ, 454, 698

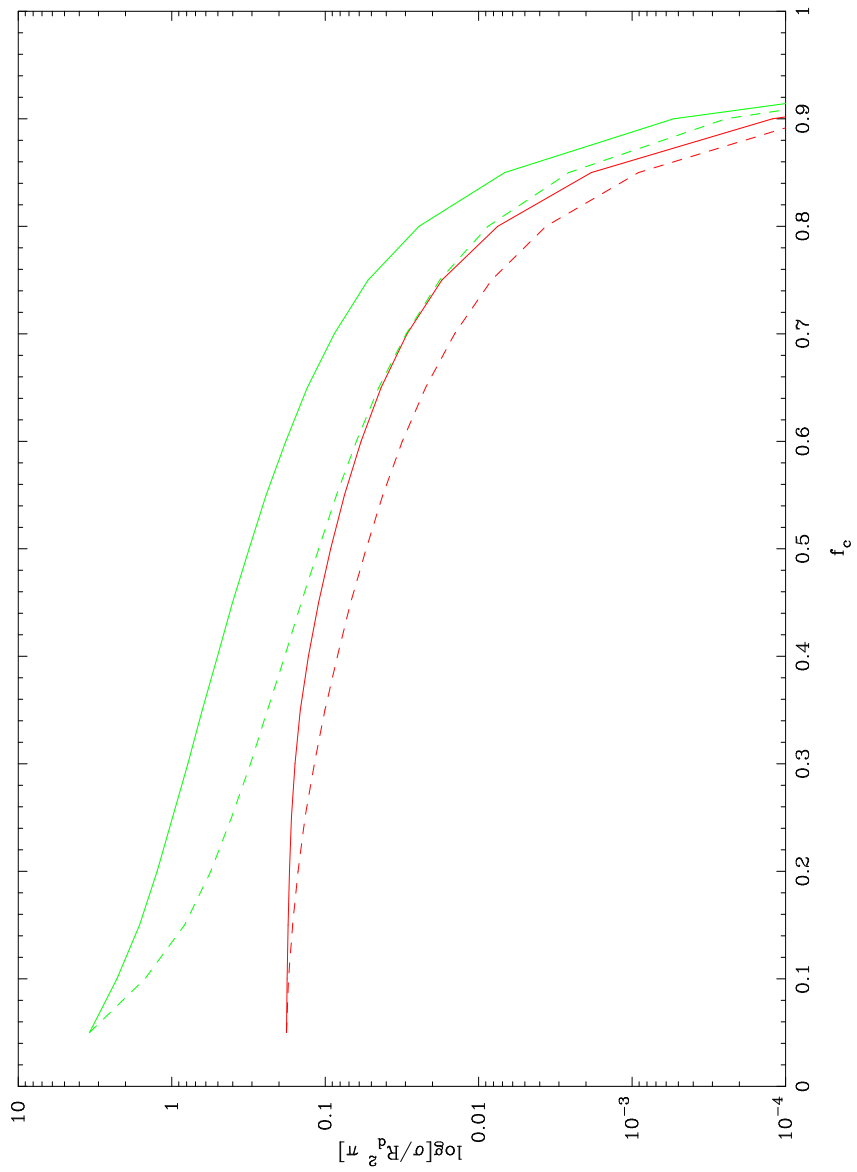


Figure 1:

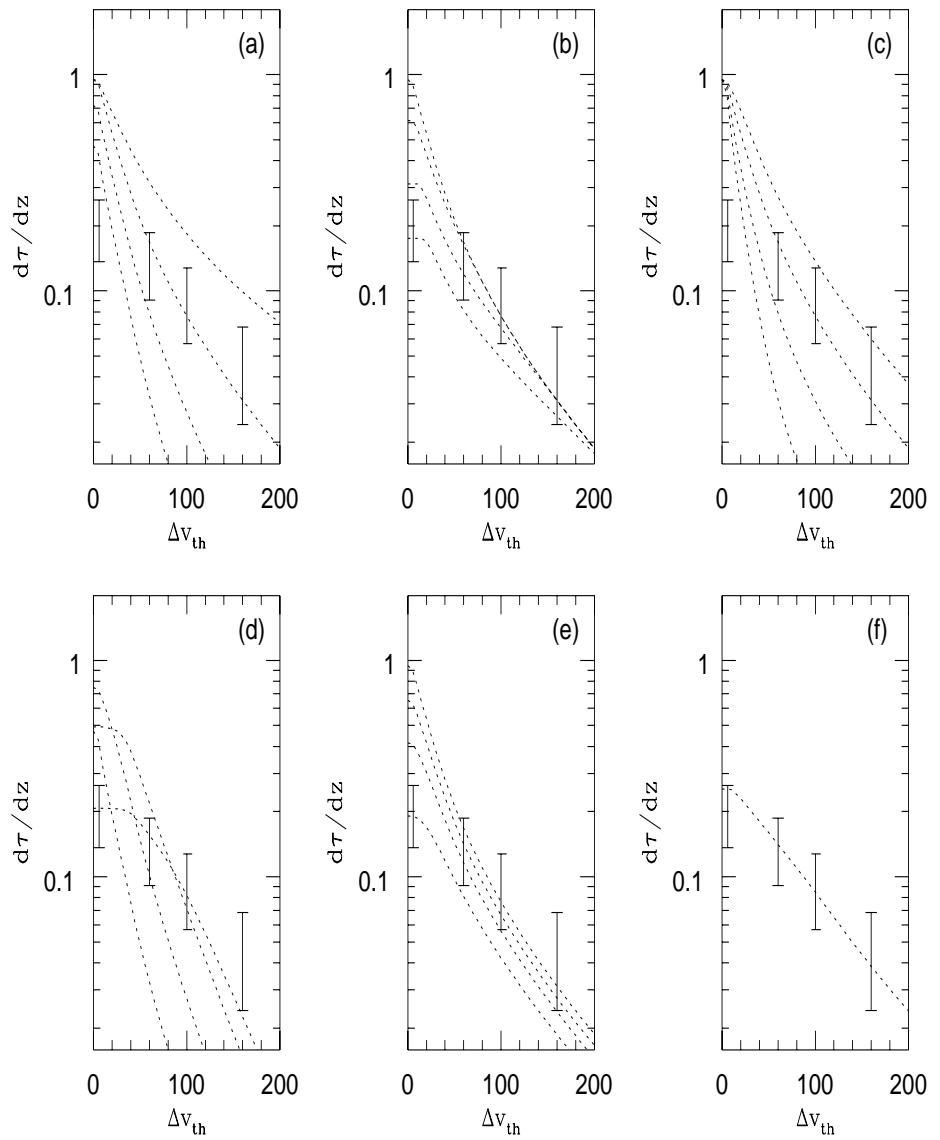


Figure 2:

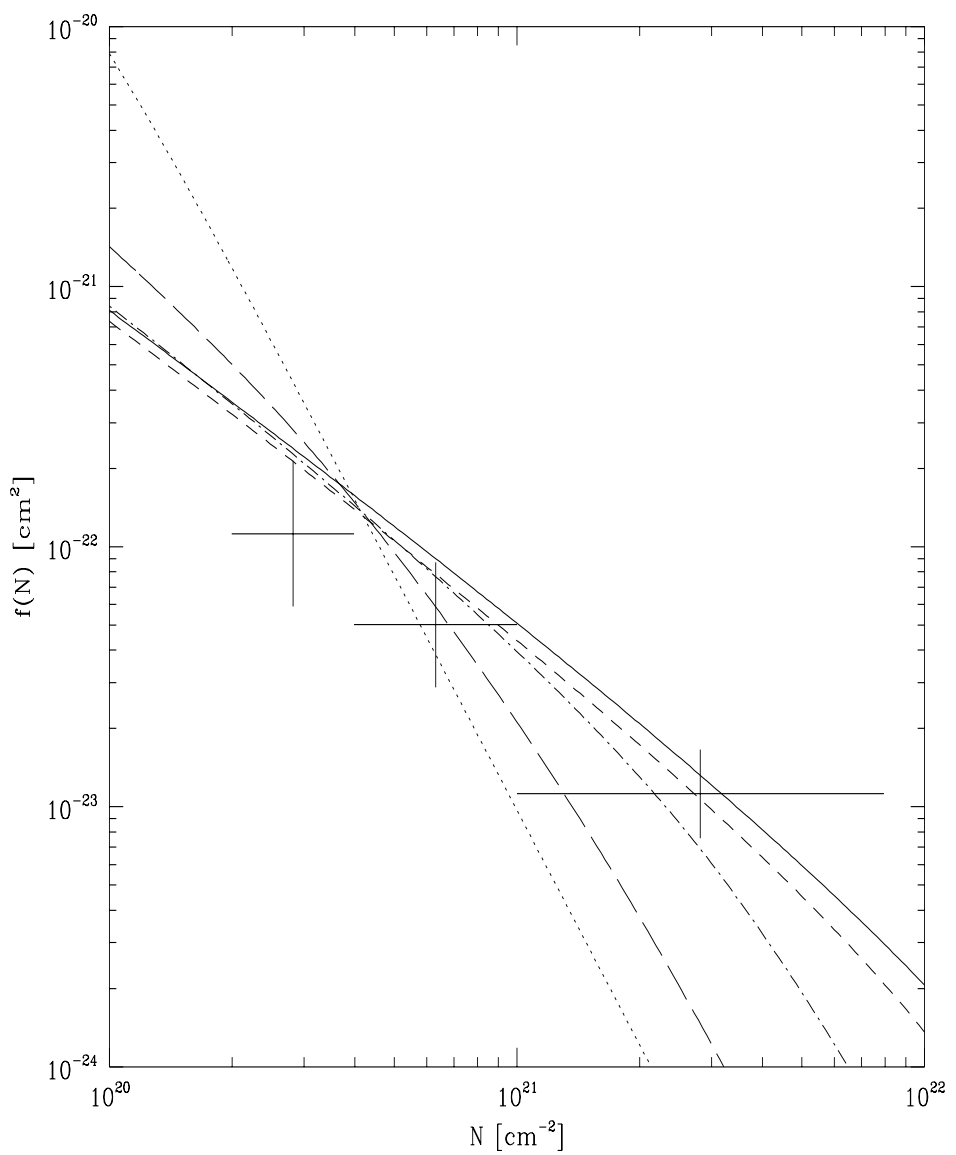


Figure 3: